Review

Ligand and metal X-ray absorption in transition metal complexes

Frank M.F. de Groot *

Inorganic Chemistry and Catalysis, Department of Chemistry, Utrecht University, Sorbonnelaan 16, 3584 CA Utrecht, Netherlands

Dedicated to Edward Solomon

Abstract

The ligand K edges and metal L edges of transition metal complexes are discussed within the perspective of recent progress in calculations on bulk transition metal oxides. Similarities and differences between bulk transition metal systems and coordination complexes are discussed. It is argued that the core hole effect reduces the amount of ligand p-states in the 3d-band (the β^2 value) by approximately 10–20%. It is suggested that matrix elements do not have to be included in XAS calculations if one calculates the projected DOS in the area of the core state radius. In case of metal L edge spectra, the additional effects of multiplets and charge transfer are discussed and compared with DFT calculations.
© 2007 Elsevier B.V. All rights reserved.

Keywords: X-ray absorption; Core hole effect; Multiplet theory; Matrix elements; Transition metal compounds

Frank de Groot *is Associate Professor in the Department of Chemistry at Utrecht University. His work reflects a concern with both the theoretical and the experimental aspects of X-ray spectroscopy, including both fundamental studies and applications. His current interest is in the use of X-ray spectroscopies for the study of the electronic and magnetic structure of condensed matter, in particular for transition metal oxides, (magnetic) nanoparticles and heterogeneous catalysts under working conditions.*

Contents

* Tel.: +31 302536763.
  E-mail address: f.m.f.degroot@uu.nl (F.M.F. de Groot).

1. Introduction

This review is written in honor of the work of Ed Solomon, in particular his elegant usage of X-ray absorption spectra of transition metal complexes [1,2]. In this contribution I discuss some of these applications and try to place them into a context of related models. The intensity of an X-ray absorption spectrum (I_{XAS}) is described with the Fermi golden rule, which in the dipole approximation reads

$$I_{XAS} \propto \sum_q |\langle \Phi_f | \hat{e}_q \cdot r | \Phi_i \rangle|^2 \delta(\hbar v - E_f + E_i) \quad (1)$$

This Fermi golden rule is a general expression and describes the transition from the initial state (Φ_i) to the final state (Φ_f) wave functions with the dipole operator $\hat{e}_q \cdot r$ summed over its different polarizations q. The delta function indicates the conservation of energy. In the single electron excitation model the initial state wave function is rewritten as a core state (c) and the final state wave function as an empty state (ε). The core hole is localized and has a well-defined energy, implying that the delta function can be reformulated with the empty orbitals or unoccupied density of states (ρ^*). This yields

$$I_{XAS} \sim M^2 \rho^* \quad (2)$$

M^2 indicates the squared matrix element and ρ^* the final state density of states (DOS). Below the final state DOS ρ^* will be compared with the ground state DOS ρ. The most popular codes to calculate the density of states of both molecules and solids are based on density functional theory. Three types of DFT codes dominate the single electron excitation simulation of X-ray absorption spectra: (a) real space multiple scattering codes such as FEFF [3], (b) pseudo-potential band structure codes such as WIEN2K [4] and paratec [5] and (c) real space quantum chemistry code, for example ADF [6] or STOBE. In the single-particle excitation model it is, implicitly, assumed that all other electrons do not participate in the X-ray induced transition and for metal L edges this model breaks down, as will be discussed below.

Central in the analysis by Ed Solomon's group is the molecular orbital picture, with the lowest unoccupied molecular orbital (LUMO) of a metal complex being described as a linear combination of metal (M_{3d}) and ligand (L_{np}) valence orbitals:

$$\Psi_{3d} = (1 - \beta^2)^{1/2} |M_{3d}\rangle + \beta^2 |L_{np}\rangle \quad (3)$$

The metal L edge excitation originates from a metal-centered 2p-orbital and only transitions to the metal-centered component of the ground state wave function have intensity. Thus, the metal L transition probes the empty metal 3d-states, and the integrated intensity of the L edge X-ray absorption spectrum can be related to the covalence $\alpha^2 [=(1 - \beta^2)]$ of the partially unoccupied 3d-orbitals in a metal complex. Similarly, the ligand K edge originates from a ligand-centered 1s-orbital and only transitions to the ligand-centered component of the ground state wave function have intensity. The integrated intensity of the K pre-edge can be related to the covalence (β^2) of the partially unoccupied 3d-orbitals. For the case of the sulfur K edge in metal sulfur systems, the Fermi golden rule is rewritten by Hedman et al. [7,8] for the lowest energy peak as

$$I_{XAS} \sim I[S(1s \rightarrow 3p)] \cdot \beta^2 = I_s \cdot \beta^2 \quad (4)$$

Here β^2 is defined as the percentage of the sulfur character and $I[S(1s \rightarrow 3p)]$ or I_s is the dipole integral. To transfer Eq. (2) to Eq. (3), M^2 can be identified with I_s and ρ^* with β^2. In this equation, β is the amount of sulfur 3p-states within the lowest unoccupied molecular orbital of the ground state wave function of a transition metal system, i.e. the empty states in the 3d-band. In case of the metal L edge, multiplet effects and charge transfer effects reorder the intensity distribution over a wider energy range. Wasinger et al. [9] used a projection method to remove these effects from the spectrum, allowing an analysis of the ground state wave function in terms of Eq. (3), with the additional advantage to separate t_{2g} and e_g symmetry states, as will be discussed below.

In this paper, I will discuss the validity of these approximations with respect to the following aspects:

1. The similarities and differences between bulk transition metal systems and coordination complexes.
2. The core hole effect and the final and initial state rules.
3. The role of the matrix elements.
4. The effect of multiplets and charge transfer.

2. Bulk transition metal systems and coordination complexes

In order to simplify the discussion, it is limited to binary transition metal systems and coordination complexes with single metal–ligand interactions. A difference between a bulk systems, say Fe_2O_3 and a coordination complex, for example $(FeCl_6)^{3-}$ is that the oxygen ion is bound to more than one iron ion. It thereby has to divide its bonding properties to more than one metal ion. In $(FeCl_6)^{3-}$ each chlorine ion is bound to only one iron ion. In addition, a bulk system has important effects from translation symmetry with small unit cell parameters. Solid $(FeCl_6)^{3-}$ systems also have periodic unit cells, but the length scales and thereby the orbital, spin, charge and magnetic correlations will be different. From the calculation point of view this favors reciprocal space calculations for bulk transition metal oxides and real space calculations for coordination complexes.

Despite these differences, the spectral shapes of both the metal L edges and the ligand K edges show many similarities in structure and behavior. A bulk transition metal oxide can also be analyzed with Eq. (3). Often one starts from the ionic limit assuming a divalent O^{2-} ion [10]. The ground state configuration is $1s^2 2s^2 2p^6$ and the $1s \rightarrow 2p$ channel is closed. The 2p-states will only be visible in ligand K edge XAS due to covalent interaction that will
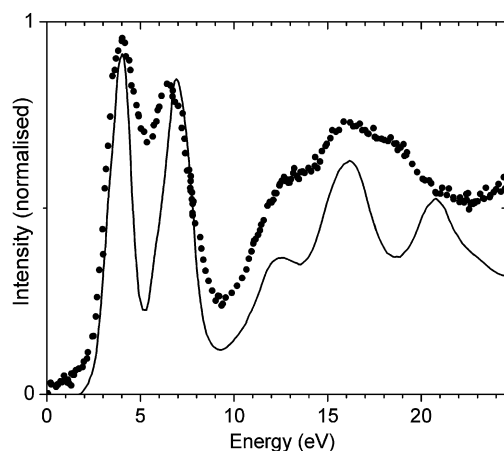
Fig. 1. Comparison between the oxygen p-projected DOS (solid) and the experimental oxygen 1s XAS spectrum (points) of rutile TiO_2 (experiment digitized from Ref. [10], theory digitized from [11]).

promote oxygen 2p character into the low-lying 3d, 4s and 4p empty states of the transition metal. Fig. 1 shows the oxygen K edge of rutile TiO_2. The first two peaks are respectively the empty t_{2g} and e_g states of the 3d-band and the second structure between 10 and 20 eV is related to the titanium 4s- and 4p-bands. It was proposed that the relative intensities of these respective bands yield the amount of oxygen 2p-states in them. Thereby the spectrum can be analyzed in the sense that there is approximately equal amount of oxygen 2p character in the t_{2g} band as in the e_g band. The e_g band has four states versus six for the t_{2g} band and in addition its energy difference with the oxygen 2p-band is larger. That its intensity is equivalent is caused by the larger overlap between oxygen 2p-states and e_g states in (distorted) octahedral systems [10]. The integrated area of the t_{2g} and e_g states together is similar to the integrated area of the metal 4sp-band, where it is assumed that matrix element effects as well as the contribution of oxygen 3p-states can be neglected (which is probably not correct). This implies that there is as much oxygen 2p–metal 3d as oxygen 2p–metal 4sp hybridization in case of TiO_2 systems. It has been shown that this 3d/4s ratio decreases with the number of empty 3d-states using the formal oxidation states. The ten 3d holes in TiO_2 yield a ratio close to 1.0, the seven holes in MnO_2 a ratio of 0.6 and the five holes in Fe_2O_3 a ratio of 0.25. This implies that the 3d hybridization decreases faster than the 4sp hybridization, which is caused by the relative localization of the 3d-states in the late transition metal oxides [10].

3. The core hole effect and the final and initial state rules

The analysis of the *ground state* wave function parameter β from an X-ray absorption spectrum is non-trivial because the spectral shape is given by the final state, at least according to the final state rule. In contrast, the initial state rule states that the integrated intensity of the XAS spectrum relates to the number of holes in the initial state.

The initial state rule follows directly from Eq. (2), writing the X-ray absorption process as an annihilation of a core electron and the creation of an extra valence electron. Integrating this equation over the complete edge and assuming that the core state is 100% occupied in the initial state, one finds that the integrated XAS spectrum yields the number of holes in a valence band. For example, in case of an L edge and assuming only 2p to 3d transitions, the integrated line strength yields the occupation of the 3d-orbitals in the ground state. In order to use the initial state rule for a particular band, one has to be able to distinguish it from other bands. In case of empty states in the 3d-band one assumes for metal L edges that the $2p \rightarrow 3d$ channel yields a (multiple peaked) white line-like spectrum, while all other channels including the $2p \rightarrow 4s$ channel yield a step-like background. This assumption is the basis used in the L edge papers of the Solomon group, where a well-defined uniform background subtraction procedure, in combination with high-quality data and normalization to a known-example together yield a firm basis [9].

However, this is not the whole story. The final state rule implies that the XAS spectral shape is determined by the final state. This also implies that the density-of-states (DOS), in other words the chemical bonding, has to be calculated in the presence of a core hole. The core hole can (and will) modify the α and β covalence parameters of the empty orbitals and due to differences in localization, this effect will be different for the 3d-states versus the 4s- and 4p-states. In other words, with XAS one determines the α^* and β^* covalence parameters of the final state and it is important to investigate if and how these values are transferable to the ground state.

The final state rule is, in contrast to the initial state rule, not a firm physical law, but instead an empirical rule based on the comparison between theory and experiment. Actually, there is much debate if the final state rule is correct and in relation to this, how to calculate the final state DOS. The present understanding of the final state rule is very incomplete, but one can at least state one conclusion that the final state rule (within a certain approximation) does not yield uniform results for metals, insulators, correlated (3d) systems and wide band systems. A typical core hole effect on a wide band system is shown in Fig. 2. This figure shows the silicon s-projected DOS of the valence band of $TiSi_2$. One observes a change of the spectral shape with intensity shifting to the lower edge of the band [12].

The usual route to calculate the final state density of states is to take a core electron out of the absorbing atom and adding the electron to the valence band. For this situation the lowest energy distribution of electrons is then calculated. In reciprocal space (band structure) calculations this implies that the excited electron is, de facto, assumed to be delocalized as far as it does not localize on the core hole impurity. Sometimes the excited electron is not implicitly included in the valence band but assumed as a background charge [4]. Because in band structure calculations one prefers the smallest possible unit cell, creating a unique
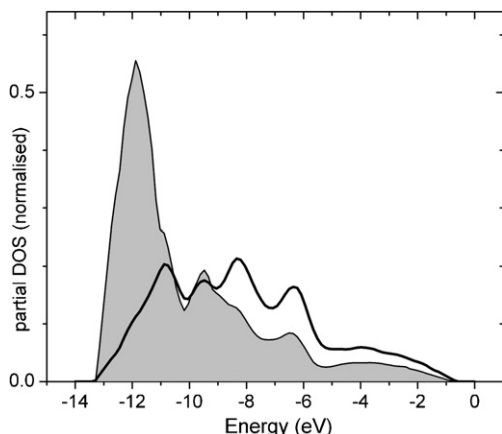
Fig. 2. Comparison between the silicon s-projected DOS in the ground state (solid) and final state (gray area) of $TiSi_2$ (digitized from Ref. [12]).

core excited atom provides a problem. The solution is to increase the unit cell until the core hole ions 'do not affect each other anymore', at least not in a way that would be visible in an XAS experiment. Assume the case of the silicon 1s core state. Instead of a silicon core and a 1s core hole, one can replace this system with a phosphorus core without a 1s core hole. This is the $Z + 1$ approximation. Several calculations for oxide solids [13] as well as for molecules, for example C_{60} [14] show that the $Z + 1$ approximation yields results that are, within the accuracy of an XAS experiment, very similar to the core excited supercell calculations.

In some case, the core excited calculation and the $Z + 1$ calculation will fail. An example is the case of $3d^9$ Cu^{II} systems such as CuO, where in the final state the 3d-hole will be filled. Within the $Z + 1$ approximation the calculation implies a Zn impurity in CuO. This Zn impurity will keep its 3d-band filled, implying that the calculated DOS will start from the empty 4sp-bands. L edge XAS experiments on Cu^{II} systems, both oxides [15] and coordination complexes [16] clearly show a sharp white line related to the 3d-hole in the initial state. This discrepancy does not imply that the final state rule is incorrect, it only implies that for $3d^9$ systems the final state rule cannot be calculated using the $Z + 1$ approximation or a core excited calculation. A more correct procedure to calculate the final state rule is to perform a number of calculations for different final states. Writing the ground state as $3d^9 4s^0$, one should calculate $2p^5 3d^{10} 4s^0$ final state and a $2p^5 3d^9 4s^1$ final state, etc. For practical calculations, one could assume a single peak for the $2p^5 3d^{10}$ final state and perform a $Z + 1$ calculation for the remainder of the spectrum.

The final state calculations of the formally $3d^{10}$ copper systems Cu metal ($3d^{10} 4s^1$) and Cu_2O ($3d^{10} 4s^2$) demonstrate two interesting situations. The WIEN2K band structure calculations of copper metal show that the best simulation of the spectral shape is found for 'a half core hole' [17]. The ground state calculation has a leading peak that is too high. This peak is reduced too much in the full

core hole calculation. The half core hole calculation exactly reproduces the experimental spectrum. The fact that the half core hole reproduces experiment is sometimes connected with the Slater transition rule. Another way of formulating this finding is that the experiment combines a ground state without core hole with a final state with a core hole, where a half core hole is an intermediate situation that apparently is best in simulating experiment. From the discussion above on $3d^9$ systems, one could also conclude that a final state band structure calculation on copper metal is essentially a Zn impurity in copper. A Zn impurity will have its 3d-states completely filled and it is the 3d character states that contribute to the leading peak.

The situation regarding the formally $3d^{10}$ system Cu_2O is also interesting. Fig. 3 shows the oxygen K edge and copper L edge spectra of Cu_2O, compared with the ground state projected DOS (bottom) and the final state DOS as calculated from a Clogston–Wolff impurity model [18]. One observes again that the core hole attracts the DOS towards the edge. Looking at the oxygen/ligand K edge one finds two similar spectra for the ground state and final state, suggesting a similar hybridization for both cases. An integration over the leading edge of the theoretical oxygen K edges between 530 eV and 535 eV yields that the final state integrated intensity is decreased by 10%. Potapov et al. [13] find a systematic decrease of the final state integrated intensity in TiO_2 and MnO. In case of TiO_2 the decrease over the 3d-band is approximately 30% (cf. Fig. 6a in Ref. [13]). Using the PARATEC code we calculated the oxygen K edge in TiO_2 and found a decrease of the 3d-band region of 20% normalized to the 4sp-band region [19]. The conclusion from these numbers is that the integrated ligand intensity in the 3d-band due to the core hole is decreased with respect to the 4sp-band and the edge jump. It is expected that this is caused by the localization of the oxygen 2p-states due to the additional core hole potential, implying a lower overlap with the 3d-states and a lower amount of ligand
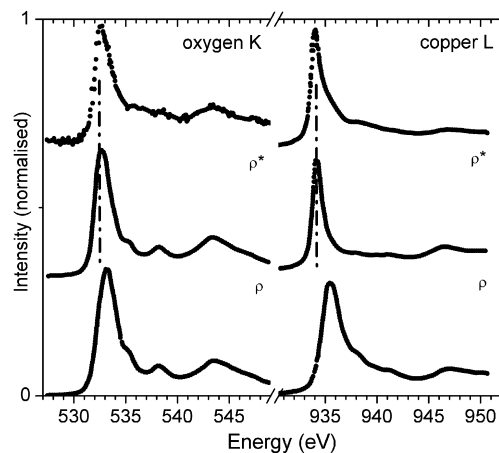

Fig. 3. Comparison between the experimental XAS spectra of the oxygen K edge (top, left) and copper L edge (top, right) of Cu_2O with the ground state DOS (bottom) and the final state DOS (middle) (digitized from Ref. [18]).

character in the 3d-band region. For the wave function analysis this implies that the values determined from XAS will be reduced with respect to the ground state. The preliminary data available suggest a reduction of 10–20%, i.e. $\beta^{2*} \sim 0.8\text{--}0.9\beta^2$. If this reduction is consistent for a series of similar systems, it can be corrected for by using reference compounds. It is noted that also the crystal field splitting is found to be consistently reduced by $\sim 10\%$ in L edge XAS with respect to the ground state [20], indicating a reduced covalence.

The situation regarding SiO_2 is different. The oxygen K edge as well as the silicon L edge increase in intensity at the white line by a factor of ~ 3 [5]. The s- and p-empty states in SiO_2 are well delocalized yielding broad bands. The core hole potential will have an effect similar to the situation drawn for $TiSi_2$ in Fig. 2 with a pile up of intensity at the bottom of the band. Because these states are very delocalized the local DOS is similar at the oxygen and the silicon site.

4. The role of matrix elements

A related issue is the role of the matrix element that describes the transition from core state to valence state. In the analysis of copper–sulfur systems, Sarangi et al. [7,8] find a large variation of the dipole integral, which could be identified with the transition matrix element. The value of I_s varies by a factor of two and scales linearly with the S 1s4p energy position. In band structure codes, the radial matrix elements are also used. The analysis of Taillefumier et al. [5] could be understood that if one calculates the core excitation only in the region of space where the core state resides, it is not necessary to include an additional matrix element. The matrix element defines the dipole selection and the fact that the transition is local, but for the remainder is a constant. The XAS intensity is derived only from the local DOS, where local has to be understood as local only in the area of the core state, defined as Ω_{R0} [5]. In this sense the transition matrix element could better be described as a projection operator to the correct spatial area. In many other band structure calculations one defines the local projected DOS in an area defined by the muffin-tin radius or the atomic sphere radius (ASA). With this definition an additional matrix element is needed to take care of the projection to the core state radius. Fig. 4 indicates the interatomic distance, assuming equal sized atoms. The muffin-tin radius is half the interatomic distance and the ASA radius is the overlapping sphere because in the ASA approximation the interstitial space is divided over the atomic radii. The core state radius Ω_{R0} is smaller than the muffin-tin radius. If the core state radius is used for the projection of the DOS, no additional matrix element is needed.

The molecular orbital picture as used to analyze the ligand K pre-edge area uses essentially delocalized orbitals for which the sulfur contribution is calculated with β^2. The radial extend of this sulfur 3p-orbital is wider than the core state radius Ω_{R0} and to correct for the spatial extend of the
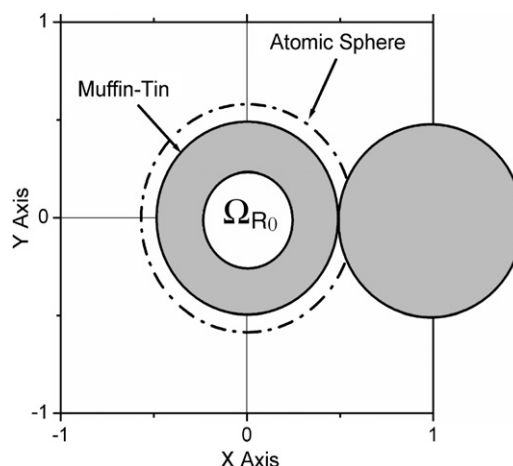

Fig. 4. Comparison of the touching muffin-tin radii, overlapping ASA radii and the small core state radius Ω_{R0}.

orbital, a dipole integral value I_s is used. This dipole integral thus effectively corrects for the amount of β^2 within the radius Ω_{R0}. Sarangi et al. [7,8] note that 'It has been shown using DFT calculations that an increase in positive charge on the absorbing S atom leads to a linear increase in the value of I_s' [21]. An increased positive charge on S increases the amount of charge of the empty 3p-states within the 3d-band in the core state radius Ω_{R0} of sulfur. This localization effect thus increases β^2 in the core excitation area with respect to the remainder of the system. As also noted by Sarangi et al. [7,8] this effect can be accounted for by increasing the dipole integral I_s. An alternative name for this integral could thus be something like the (sulfur 3p) localization factor. X-ray absorption spectra of the ligand site and the metal site thus both probe only a small core state radius Ω_{R0} region around the respective nuclei. The extrapolation to the complete delocalized molecular orbitals is taken care of by the dipole integral/localization factor. It would be very interesting to compare the ground state and final state DOS results as a function of the radius, changing it from below the core state radius Ω_{R0} to values above the muffin-tin radius. Effectively this yields the real space variations of the empty states and understanding their behavior in detail would improve our understanding of XAS spectra, implying a more detailed and quantitative usage of XAS for applications.

5. The effect of multiplets and charge transfer

In case of metal L edges, multiplet effects and charge transfer effects are further complicating the analysis [22–24]. The wave function of the core hole interacts with the valence holes and these atomic interactions turn out to be essentially unscreened in the solid state. In addition to multiplet effects, metal L edges are subject to screening effects that involve localized electron states. These screening effects can be treated with the charge transfer model and the combination of both effects has lead to the development of the charge transfer multiplet (CTM) model. In case of
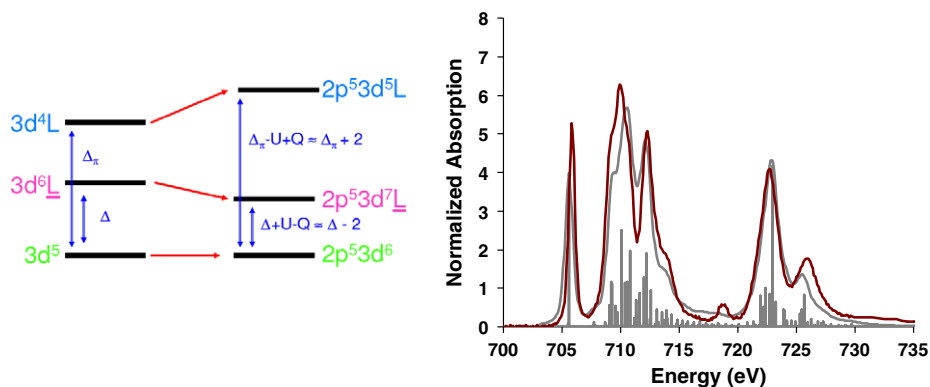
Fig. 5. (Left) The mixing of a $3d^5$ ground state with $3d^6\underline{L}$ at energy Δ and with $3d^4L$ at energy Δ_π. The final state energies shift down for CT and up for MLCT by a small energy, given as the difference between the core hole potential Q and the Hubbard U. (right) The experimental L edge spectra of $Fe^{III}(CN)_6$ (thick line) compared with CTM calculations (sticks and broadened to thin line).

X-ray absorption, charge transfer effects are only important in systems with a high valence, which is beautifully demonstrated by Sarangi et al for Cu^{III} coordination complexes [16] and Hu et al. for Cu^{III} oxides [25,26].

In collaboration with Erik Wasinger and Rosalie Hocking from Ed Solomon's group, the CTM method has been analyzed to derive the nature of the ground state, also in order to compare it to the ground states used in DFT calculations. In transition metal systems with only ligand to metal charge transfer, it is sufficient to describe the initial state as $3d^n + 3d^{n+1}\underline{L}$. A $3d^5$ low-spin ground state has five t_{2g} states filled (one empty) and all e_g states empty. t_{2g}-mixing leads to a $t_{2g}^6\underline{L}$-configuration, which has one multiplet state and e_g-mixing leads to $t_{2g}^5e_g^1\underline{L}$, which can have a large range of multiplet states. It turns out that in case of $Fe^{III}(tacn)_2$ the contribution of t_{2g}-mixing is only a few percent, versus 37% for e_g-mixing [9].

In systems that contain significant ligand metal charge transfer (LMCT) as well as metal ligand charge transfer (MLCT), this has to be included explicitly. Fig. 5 shows the combined mixing of $3d^5 + 3d^6\underline{L} + 3d^4L$. The $3d^6\underline{L}$ configuration takes care of the LMCT and $3d^4L$ relates to LMCT effects such as π-backbonding. The creation of a 2p core hole transfers the extra electron to the 3d-band, which is essentially a charge conserving optical transition. This implies that the ordering of states remains similar to the ground state, where it is noticed that each $3d^n$ configuration consists of the full crystal field multiplet manifold. In addition, the final state $2p^53d^n$ configurations contain the effects of the 2p spin–orbit coupling and the 2p3d multiplet effects. This methodology is able to describe π-bonding and has been used to describe the L edge spectra of $Fe^{III}(CN)_6$ and $Fe^{II}(CN)_6$ [27]. The use of a ground state that is a mixture of $3d^5 + 3d^6\underline{L} + 3d^4L$ is also important for iron-heme systems as was analyzed by Hocking et al. [28].

6. Concluding remarks

I hope that with this review on the usage of ligand K and metal L edge XAS spectra, I have provided a number of ideas in order to further develop the analysis methods as derived by Ed Solomon and his coworkers. Several issues regarding XAS spectra are not yet well understood. Matrix elements play a role of transferring the empty states within the core hole radius to the complete wave function. The precise nature of core hole effects in various systems is, as yet, not well understood. It would be useful to derive some general rules to estimate core hole effects quantitatively. The metal L edge spectra are nowadays well understood, but a more direct link to ab initio DFT theory would be important.

Acknowledgement

References

[1] E.I. Solomon, B. Hedman, K.O. Hodgson, A. Dey, R.K. Szilagyi, Coord. Chem. Rev. 249 (2005) 97.
[2] T. Glaser, B. Hedman, K.O. Hodgson, E.I. Solomon, Acc. Chem. Res. 33 (2000) 859.
[3] A.L. Ankudinov, B. Ravel, J.J. Rehr, S.D. Conradson, Phys. Rev. B 58 (1998) 7565.
[4] C. Hebert, Micron 38 (2007) 12.
[5] M. Taillefumier, D. Cabaret, A.M. Flank, F. Mauri, Phys. Rev. B 66 (2002) 195107.
[6] E.J. Baerends, D.E. Ellis, P. Ros, Chem. Phys. 2 (1973) 41.
[7] B. Hedman, K.O. Hodgson, E.I. Solomon, J. Am. Chem. Soc. 112 (1990) 1643.
[8] R. Sarangi, S.D. George, D.J. Rudd, R.K. Szilagyi, X. Ribas, C. Rovira, M. Almeida, K.O. Hodgson, B. Hedman, E.I. Solomon, J. Am. Chem. Soc. 129 (2007) 2316.
[9] E.C. Wasinger, F.M.F. de Groot, B. Hedman, K.O. Hodgson, E.I. Solomon, J. Am. Chem. Soc. 125 (2003) 12894.
[10] F.M.F. de Groot, M. Grioni, J.C. Fuggle, J. Ghijsen, G.A. Sawatzky, H. Petersen, Phys. Rev. B 40 (1989) 5715.
[11] F.M.F. de Groot, J. Faber, J.J.M. Michiels, M.T. Czyzyk, M. Abbate, J.C. Fuggle, Phys. Rev. B 48 (1993) 2074.
[12] P.J.W. Weijs, M.T. Czyzyk, J.F. Vanacker, W. Speier, J.B. Goedkoop, H. Vanleuken, H.J.M. Hendrix, R.A. Degroot, G. Vanderlaan, K.H.J. Buschow, G. Wiech, J.C. Fuggle, Phys. Rev. B 41 (1990) 11899.

[13] P.L. Potapov, K. Jorissen, D. Schryvers, D. Lamoen, Phys. Rev. B 70 (2004) 045106.

[14] M. Nyberg, Y. Luo, L. Triguero, L.G.M. Pettersson, H. Agren, Phys. Rev. B 60 (11) (1999) 7956.

[15] M. Grioni, M.T. Czyzyk, F.M.F. de Groot, J.C. Fuggle, B.E. Watts, Phys. Rev. B 39 (8) (1989) 4886.

[16] R. Sarangi, N. Aboelella, K. Fujisawa, W.B. Tolman, B. Hedman, K.O. Hodgson, E.I. Solomon, J. Am. Chem. Soc. 128 (25) (2006) 8286.

[17] J. Luitz, M. Maier, C. Hebert, P. Schattschneider, P. Blaha, K. Schwarz, B. Jouffrey, Eur. Phys. J. B 21 (3) (2001) 363.

[18] M. Grioni, J.F. Vanacker, M.T. Czyzyk, J.C. Fuggle, Phys. Rev. B 45 (1992) 3309.

[19] I. Swart, D. Cabaret, F.M.F. de Groot, 2007, unpublished.

[20] S.P. Cramer, F.M.F. Degroot, Y. Ma, C.T. Chen, F. Sette, C.A. Kipke, D.M. Eichhorn, M.K. Chan, W.H. Armstrong, E. Libby, G. Christou, S. Brooker, V. McKee, O.C. Mullins, J.C. Fuggle, J. Am. Chem. Soc. 113 (21) (1991) 7937.

[21] F. Neese, B. Hedman, K.O. Hodgson, E.I. Solomon, Inorg. Chem. 38 (21) (1999) 4854.

[22] F.M.F. de Groot, J.C. Fuggle, B.T. Thole, G.A. Sawatzky, Phys. Rev. B 42 (1990) 5459.

[23] F.M.F. de Groot, J.C. Fuggle, B.T. Thole, G.A. Sawatzky, Phys. Rev. B 41 (1990) 928.

[24] F.M.F. de Groot, Coord. Chem. Rev. 249 (2005) 31.

[25] Z. Hu, G. Kaindl, S.A. Warda, D. Reinen, F.M.F. de Groot, B.G. Muller, Chem. Phys. 232 (1998) 63.

[26] Z. Hu, C. Mazumdar, G. Kaindl, F.M.F. de Groot, S.A. Warda, D. Reinen, Chem. Phys. Lett. 297 (3–4) (1998) 321.

[27] R.K. Hocking, E.C. Wasinger, F.M.F. de Groot, K.O. Hodgson, B. Hedman, E.I. Solomon, J. Am. Chem. Soc. 128 (32) (2006) 10442.

[28] R.K. Hocking, E.C. Wasinger, Y.L. Yan, F.M.F. deGroot, F.A. Walker, K.O. Hodgson, B. Hedman, E.I. Solomon, J. Am. Chem. Soc. 129 (2007) 113.